J Fluoresc
DOI 10.1007/s10895-014-1370-7

ORIGINAL PAPER

Location of Novel Benzanthrone Dyes in Model Membranes as Revealed by Resonance Energy Transfer

Olga Zhytniakivska · Valeriya Trusova · Galyna Gorbenko · Elena Kirilova · Inta Kalnina · Georgiy Kirilov · Julian Molotkovsky · Jukka Tulkki · Paavo Kinnunen

Received: 25 November 2013 / Accepted: 24 February 2014
© Springer Science+Business Media New York 2014

Abstract Förster resonance energy transfer (FRET) between anthrylvinyl-labeled phosphatidylcholine (AV-PC) as a donor and newly synthesized benzanthrones (referred to here as A8, A6, AM12, AM15 and AM18) as acceptors has been examined to gain insight into molecular level details of the interactions between benzanthrone dyes and model lipid membranes composed of zwitterionic lipid phosphatidylcholine and its mixtures with anionic lipids cardiolipin (CL) and phosphatidylglycerol (PG). FRET data were quantitatively analyzed in terms of the model of energy transfer in two-dimensional systems taking into account the distance dependence of orientation factor. Evidence for A8 location in phospholipid headgroup region has been obtained. Inclusion of CL and PG into PC bilayer has been found to induce substantial relocation of A6, AM12, AM15 and AM18 from hydrophobic membrane core to lipid-water interface.

O. Zhytniakivska · V. Trusova · G. Gorbenko
Department of Nuclear and Medical Physics, V.N. Karazin Kharkiv National University, 4 Svobody Sq., Kharkiv 61077, Ukraine

E. Kirilova · I. Kalnina · G. Kirilov
Department of Chemistry and Geography, Faculty of Natural Science and Mathematics, Daugavpils University, 13 Vienibas, Daugavpils LV5401, Latvia

J. Molotkovsky
Institute of Bioorganic Chemistry, Russian Academy of Science, 16/10 Miklukho-Maklaya, Moscow 117871, Russia

J. Tulkki · P. Kinnunen
Department of Biomedical Engineering and Computational Science, School of Science and Technology, Aalto University, FI-00076 Espoo, Finland

O. Zhytniakivska (✉)
52-52 Tobolskaya Str., Kharkiv 61072, Ukraine
e-mail: olya_zhitniakivska@yahoo.com

Published online: 05 March 2014

Keywords Benzanthrone dyes · Lipid membranes · Resonance energy transfer

Introduction

The group of benzanthrone dyes attracts growing attention from a biomedical point of view since the pioneering works of Dobretsov & Vladimirov in the 1970s, who demonstrated that 3-methoxybenzanthrone (MBA) responds to the membrane structural changes produced by the shifts in cholesterol level, temperature, pH, etc. [1]. Subsequently, Yang et al. reported that MBA displays DNA intercalation properties [2]. Furthermore, it was shown that benzanthrone derivatives possess marked sensitivity to the alterations in immune status of a human organism at different pathologies [3, 4]. Likewise, aminobenzanthrone dyes turned out to be suitable for characterizing protein oligomeric species and highly ordered pathogenic aggregates, amyloid fibrils [5, 6]. The advantageous photophysical properties of benzanthrones include (i) large extinction coefficients; (ii) marked Stokes shift; (iii) very weak fluorescence in an aqueous phase; (iv) ability to intramolecular charge transfer (ICT) from amine substituent to carbonyl group [7–9]. It is generally known that spectral behavior of the dyes emitting from ICT state (e.g., Laurdan, Prodan, Nile Red, NBD-and anthroyl-derivatives) strongly depends on physicochemical characteristics of fluorophore environment (polarity, viscosity, formation of hydrogen bonds or other intermolecular interactions) [10]. Due to their capability to form ICT state, benzanthrones also belong to the group of environment-sensitive probes which are especially relevant for membrane studies.

In our recent works we evaluated the lipid-associating ability of some amino- and amidinobenzanthrones [11, 12]. Fluorimetric determination of partition coefficients allowed us to conclude that amidinoderivatives exhibit stronger

membrane partitioning compared to aminobenzanthrones [12]. Likewise, it was found that spectral responses of the two aminoderivatives can be correlated with bilayer hydration [11]. These findings give an impetus for further characterization of benzanthrones as promising fluorescent probes for exploring membrane-related processes. In this regard, determining the precise position of these dyes in a membrane seems to be crucial for their practical applicability. To the best of our knowledge, the exact depth at which benzanthrones reside within a lipid bilayer is still unknown.

To fill this gap, in the present study we employed Förster resonance energy transfer (FRET) technique to determine the location of these dyes in the model membranes composed of zwitterionic lipid phosphatidylcholine and its mixtures with anionic lipids cardiolipin (CL) and phosphatidylglycerol (PG). Anthrylvinyl-labeled phosphatidylcholine was recruited as the energy donor with benzanthrone moiety being the acceptor. To evaluate the fluorophore position relative to lipid bilayer midplane, FRET data were quantitatively analyzed in terms of the modified Fung & Stryer model [13] describing energy transfer in two-dimensional systems.

Experimental

Materials

Bovine heart cardiolipin (CL), 1-palmitoyl-2-oleoyl-*sn*-glycero-3-phosphocholine (PC) and 1-palmitoyl-2-oleoyl-*sn*-glycero-3-phospho-*rac*-glycerol (PG) were from Avanti Polar Lipids (Alabaster, AL). Fluorescent lipid, 1-acyl-2-[12-(9-antryl)-11*E*-dodecenoyl]-*sn*-glycero-3-phosphocholine (AV-PC) was synthesized as described previously [14, 15]. Benzanthrone dyes AM12, AM15, AM18, A6 and A8 (Fig. 1) were synthesized at the Faculty of Natural Sciences and Mathematics of Daugavpils University as described in detail elsewhere [7, 16]. All other chemicals were of analytical grade and used without further purification.

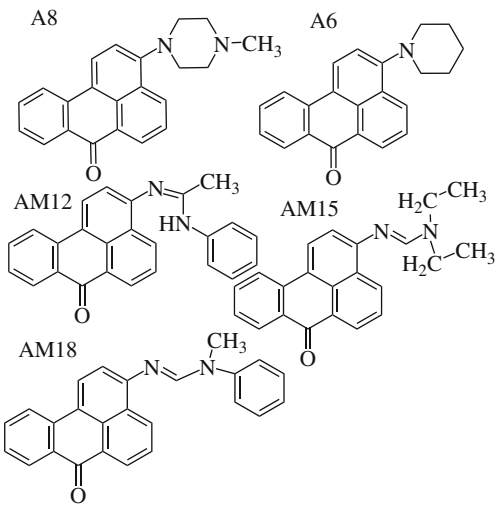

Fig. 1 Chemical structure of the examined benzanthrone dyes

Preparation of Lipid Vesicles

Lipid vesicles composed of PC and PC mixtures with CL or PG were prepared using the extrusion technique. A thin lipid film was first formed of the lipid mixtures in chloroform by removing the solvent under a stream of nitrogen. The dry lipid residues were subsequently hydrated with 20 mM HEPES, 0.1 mM EDTA, pH 7.4 at room temperature to yield lipid concentration of 1 mM. Thereafter, lipid suspension was extruded through a 100 nm pore size polycarbonate filter (Millipore, Bedford, USA). In this way, six types of lipid vesicles containing PC and 5.3, 11.1 or 25 mol% CL, and 20 or 40 mol% PG were prepared, with the content of phosphate being identical for all liposome preparations. Hereafter, liposomes containing 20 or 40 mol% PG are referred to as PG20 or PG40, while liposomes bearing 5.3, 11.1, or 25 mol% CL are denoted as CL5, CL11 or CL25, respectively. Fluorescent lipid analogue AV-PC (0.3 mol% of total lipid), used here as an energy donor, was added to the lipid mixture prior to the solvent evaporation. The concentration of fluorescent lipid was determined spectrophotometrically using anthrylvinyl extinction coefficient $E_{367}=9\times10^3$ M^{-1} cm^{-1} [14].

Fluorescence Measurements

Fluorescence measurements were performed with LS-55 spectrofluorimeter (Perkin Elmer Ltd., Beaconsfield, UK) equipped with magnetically stirred, thermostated cuvette holder at 25 °C. 20 μL of the stock solution (1 mM) of anthrylvinyl-doped liposomes were added to 1.98 mL of phosphate buffer (pH 7.4) and further titrated by benzanthrone dyes, to vary acceptor concentration. AV-PC emission spectra were recorded with 367 nm excitation wavelength. Excitation and emission slit widths were set at 10 nm. Fluorescence intensity measured in the presence of benzanthrone dyes at the maximum of AV emission (430 nm) was corrected for reabsorption and inner filter effects using the following coefficients [17]:

$$k_{corr}=\frac{\left(1-10^{-A_0^{ex}}\right)\left(A_0^{ex}+A_a^{ex}\right)\left(1-10^{-A_0^{em}}\right)\left(A_0^{em}+A_a^{em}\right)}{\left(1-10^{-\left(A_0^{ex}+A_a^{ex}\right)}\right)A_0^{ex}\quad\left(1-10^{-\left(A_0^{em}+A_a^{em}\right)}\right)A_0^{em}} \quad (1)$$

where A_0^{ex}, A_0^{em} are the donor optical densities at the excitation and emission wavelengths in the absence of acceptor, A_a^{ex}, A_a^{em} are the acceptor optical densities at the excitation and emission wavelengths, respectively.

Fluorescence anisotropy measurements were conducted with the following excitation (λ_{ex}) and emission (λ_{em})

wavelengths: (λ_{ex}=440 nm, λ_{em}=587–592 nm for A8 (depending on liposome composition); λ_{ex}=450 nm, λ_{em}=593 nm for A6; λ_{ex}=470 nm, λ_{em}=582 nm for AM12; λ_{ex}=480 nm, λ_{em}=574 nm for AM15; λ_{ex}=460 nm, λ_{em}=570 nm for AM18) and AV-PC (λ_{ex}=367 nm, λ_{em}=430 nm).

Theoretical Background

Partition Model

The binding of benzanthrone dyes to model membranes has been analyzed in terms of partition model [18]. The total concentration of the dye distributing between aqueous and lipid phases (Z_{tot}) can be represented as:

$$Z_{tot} = Z_F + Z_L \tag{2}$$

where subscripts F and L denote free and lipid-bound dye, respectively. The coefficient of dye partitioning between the two phases (K_P) is defined as:

$$K_P = \frac{Z_L V_W}{Z_F V_L} \tag{3}$$

here V_W, V_L are the volumes of the aqueous and lipid phases, respectively. Given that under the employed experimental conditions the volume of lipid phase is much less than the total volume of the system V_t, we assume that $V_W \approx V_t$=1 dm^3. It is easy to show that

$$Z_F = \frac{Z_{tot} V_W}{V_W + K_P V_L} = \frac{Z_{tot}}{1 + K_P V_L} \tag{4}$$

The dye fluorescence intensity measured at a certain lipid concentration can be written as:

$$I = a_f Z_F + a_L Z_L = Z_F\left(a_f + a_L \frac{K_P V_L}{V_W}\right) = Z_F\left(a_f + a_L K_P V_L\right) \tag{5}$$

where a_f, a_L represent molar fluorescence of the dye free in solution and in a lipid environment, respectively. From the Eqs. (4) and (5) one obtains:

$$I = \frac{Z_{tot} V_W \left(a_f + a_L K_P V_L\right)}{V_W + K_P V_L} \tag{6}$$

The volume of lipid phase can be determined from:

$$V_L = N_A C_L \sum v_i f_i \tag{7}$$

Where C_L is the molar lipid concentration, f_i is mole fraction of the i-th bilayer constituent, v_i is its molecular volume taken as 1.58 nm^3, 3 nm^3 and 2.8 nm^3 for PC, CL and PG respectively [19]. The relationship between K_p and fluorescence intensity increase (ΔI) upon the dye transfer from water to lipid phase can be written as [18]:

$$\Delta I = I_L - I_W = \frac{K_p V_L (I_{\max} - I_W)}{1 + K_p V_L} \tag{8}$$

where I_L is the dye fluorescence intensity measured at a certain lipid concentration C_L, I_W is the dye fluorescence intensity in a buffer, $I_{\max}$ is the limit fluorescence in a lipid environment.

Model of Resonance Energy Transfer

In analyzing the FRET data presented here we considered the lipid-protein systems as containing one acceptor plane located at a distance d_c from the membrane center and two donor planes separated by a distance d_t (Fig. 2). Given that for the outer donor plane d_a=$|d_c$−0.5$d_t|$ while for the inner plane d_a=d_c+0.5d_t, the following relationships hold [20]:

$$S_1(\lambda) = \int_{|d_c - 0.5 d_t|}^{\infty} \left[1 - \exp\left(-\lambda \kappa_1^2(R)\left(\frac{R_o^r}{R}\right)^6\right)\right] 2\pi R dR \tag{9}$$

$$S_2(\lambda) = \int_{d_c + 0.5 d_t}^{\infty} \left[1 - \exp\left(-\lambda \kappa_2^2(R)\left(\frac{R_o^r}{R}\right)^6\right)\right] 2\pi R dR \tag{10}$$

$$\kappa_{1,2}^2(R) = \langle d_D^x \rangle \langle d_A^x \rangle \left(3\left(\frac{d_c \mp 0.5 d_t}{R}\right)^2 - 1\right) + \frac{1 - \langle d_D^x \rangle}{3} + \frac{1 - \langle d_A^x \rangle}{3} + \left(\frac{d_c \mp 0.5 d_t}{R}\right)^2 \left(\langle d_D^x \rangle - 2\langle d_D^x \rangle \langle d_A^x \rangle + \langle d_A^x \rangle\right) \tag{11}$$

$$Q_r = 0.5 \times \left(\int_0^{\infty} \exp(-\lambda) \exp\left[-C_a^s S_1(\lambda)\right] d\lambda + \int_0^{\infty} \exp(-\lambda) \exp\left[-C_a^s S_2(\lambda)\right] d\lambda \right) \tag{12}$$

where S_1 and S_2 are the quenching contributions describing energy transfer to the outer and inner donor planes, respectively; $\langle d_D^x \rangle$ and $\langle d_A^x \rangle$ are so-called axial depolarization factors; $\lambda = t/\tau_d$, τ_d is the lifetime of excited donor in the

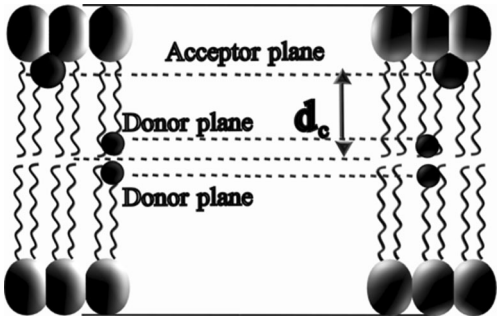

Fig. 2 Schematic representation for relative bilayer positions donors (anthrylvinyl moiety of AV-PC) and acceptors (benzanthrones) in the model membranes

absence of acceptor; R_o is the Förster radius; Q_r is the relative quantum yield of a donor; C_a^s is the concentration of acceptors per unit area; κ^2 is an orientation factor. When the donor and acceptor planar arrays are located at different levels across the membrane, multiple donor-acceptor pairs are involved in energy transfer, so that orientation factor appears to be a function of the donor-acceptor separation (R). The relationships (9)–(12) are valid when the donor and acceptor transition moments are distributed about the axes D_x and A_x parallel to the bilayer normal N. If this is not the case, additional depolarization factors accounting for the deviations of D_x and A_x from N should be introduced: $d^a_{D,A} = \frac{3}{2}\cos^2\alpha_{D,A} - \frac{1}{2}$, where $\alpha_{D,A}$ are the angles made by D_x and A_x with N. By applying the Soleillet's theorem stating the multiplicativity of depolarization factors, Eq. (11) may be rewritten in a more general form:

$$\kappa^2_{1,2}(R) = d_D d_A\left(3\left(\frac{d_c \mp 0.5d_t}{R}\right)^2 - 1\right) + \frac{1-d_D}{3} + \frac{1-d_A}{3} + \left(\frac{d_c \mp 0.5d_t}{R}\right)^2 (d_D - 2d_D d_A + d_A) \quad (13)$$

where $d_{D,A} = \langle d^x_{D,A}\rangle d^a_{D,A}$.

Results and Discussion

Our recent research revealed high sensitivity of benzanthrone fluorescence parameters to the changes in physicochemical properties of the model membranes produced by inclusion of anionic lipid cardiolipin and cholesterol into phosphatidylcholine bilayer [11]. In the previous experiments we employed rather small CL concentrations (5 and 10 mol%), characteristic of the inner mitochondrial membrane. In the present study we extend our investigation to another anionic lipid phosphatidylglycerol (20 mol%, since physiological concentration of PG in membranes does not exceed 20 mol%). However, it is known that CL concentration can be as high as 25–30 % of total lipid mass at contact sites where the inner and outer mitochondrial membranes interact [21]. To clarify, to what extent electrostatics is essential for lipid bilayer interactions of benzanthrone dyes, we found it reasonable to perform model experiments with CL (25 mol%) and PG (40 mol%) concentrations exceeding physiological ones.

Since the application of fluorescent probes for monitoring membrane processes requires knowing of not only their binding properties, but also fluorophore localization in a lipid bilayer, the present study was focused mainly on evaluating the depth of bilayer penetration of the newly synthesized amino (A8 and A6) and amidino (AM12, AM15 and AM18) benzanthrones in the model membranes of various composition.

Analysis of the $\Delta I(C_L)$ dependencies in terms of the above partition model (Eqs. (2)–(8)) yielded partition coefficients of benzanthrones in different lipid systems. As seen in Table 1, inclusion of CL or PG into PC bilayer gives rise to the increase in the K_P values for A8, whereas A6, AM12, AM15 and AM18 display the opposite behavior. According to modern theories of membrane electrostatics, the partition coefficient is a quantity depending on both electrostatic and nonelectrostatic terms [22–24]:

$$K_p = \exp\left(-\{w_{el} + w_{born} + w_h + w_n + w_d\}/kT\right) \quad (14)$$

where w_{el} characterizes coulombic ion-membrane interactions, w_{born} contributions corresponds to the Gibbs energy of charge transfer between the regions of differing properties, w_h is the term which reflects a number of phenomena concerned with the membrane hydration, w_n is the neutral energy contribution, including hydrophobic, van der Waals and steric factors and w_d accounts for the membrane dipole potential. In the case of uncharged benzanthrone dyes, the contributions of the first two electrostatic factors seem to be negligible, so that the dye partitioning into lipid phase is controlled predominantly by the other terms. Moreover, taking into account the differences between partition behavior of A8 on one hand and A6, AM12, AM15, AM18 on the other hand, relative significance of these terms seems to be different for various dyes under study. Of special interest in this regard is the ability of benzanthrone dyes to form hydrogen bonds (due to the presence of carbonyl group in their structure) with structural groups of lipid membranes as well as with water molecules at different depth inside the bilayer. It is known, that photophysical properties of benzanthrone dyes strongly depend on the electron donor-acceptor interactions within chromophoric system [7–9]. The occurrence of ICT state is controlled by electron-donating and electron-accepting powers of the fluorophore functional groups. In this case hydrogen bonding can exert effect on charge transfer character of benzanthrone dyes, thereby changing their photophysical and partition properties. It has been previously demonstrated that radiationless deactivation (via internal conversion, photoinduced electron transfer, intermolecular charge transfer, etc.)

Table 1 Partition coefficients of benzanthrone dyes in different lipid systems

Membrane composition	Partition coefficient, $K_p \times 10^4$				
	A8	A6	AM12	AM15	AM18
PC	0.9±0.07	11±1.5	18±0.8	6.1±0.2	12±0.8
	(0.19)	(0.21)	(0.24)	(0.20)	(0.20)
CL5	3.4±0.05	9.2±0.9	8.7±0.3	2.7±0.2	9.7±0.6
	(0.17)	(0.22)	(0.26)	(0.22)	(0.23)
CL11	6.2±1.6	8.4±0.7	5.8±0.6	1.6±0.5	7.7±0.5
	(0.19)	(0.24)	(0.27)	(0.23)	(0.25)
CL25	7.8±0.5	7.8±0.5	3.1±0.8	1.4±0.4	5.4±0.7
	(0.22)	(0.23)	(0.28)	(0.24)	(0.26)
PG20	5.3±0.7	8.2±0.3	7.9±0.4	3.4±0.5	6.9±0.5
	(0.19)	(0.21)	(0.27)	(0.21)	(0.23)
PG40	8.1±0.9	7.1±1.1	5.6±0.5	2.9±0.8	3.7±0.6
	(0.21)	(0.23)	(0.27)	(0.22)	(0.21)
Lipophilicity	4.21	6.27	7.18	5.42	6.57

Shown in parentheses are fluorescence anisotropy values of benzanthrone dyes

can be dramatically influenced by hydrogen-bonding interactions through modulation of electronic states [25–27]. Furthermore, it is the substitution in C-3 position of benzanthrone dyes that determines the differences in their behaviour. Likewise, hydrogen bonding ability of benzanthrone dyes may affect resonance energy transfer profile through orientation factor. However, taking into account that in the employed RET model orientation factor depends on the donor-acceptor distance and the donor and acceptor transition moments are supposed to be distributed within the cones about the axes D_x and A_x parallel to the bilayer normal. Importantly, the half-angles of these cones were estimated from the experimentally measured depolarization factors. This implies that all possible kinds of dye-lipid interactions, including hydrogen bonding, which determine fluorophore mobility in a lipid bilayer (that manifests itself in the value of depolarization factor) are actually allowed for as implicit parameters in our RET model.

It should be noted that the obtained K_P estimates were further used to calculate surface concentration of benzanthrones according to Eq. (11), thereby creating prerequisites for quantitative interpretation of FRET data.

As seen in Fig. 3, FRET between AV-PC as a donor and benzanthrone dye as an acceptor manifested itself in the progressive decrease of AV fluorescence intensity and, accordingly, relative quantum yield, with increasing the dye concentration. AV-PC emission spectrum overlaps with absorption spectrum of benzanthrones, resulting in Förster radii 3.1 nm, 2.9 nm, 2.7 nm, 3.2 nm and 2.5 nm for A8, A6, AM12, AM15 and AM18, respectively. Presented in Fig. 4 are the relative quantum yields of AV-PC plotted against the concentration of bound dye for different types of liposomes.

The results of FRET measurements were quantitatively analyzed within the framework of the above theoretical model (Eqs. (9)–(13)). The fitting of this model to the experimental dependencies of relative quantum yield on concentration of bound dye (Fig. 4) allowed us to evaluate the distance between the acceptor plane and bilayer center (d_c). The value of d_c was estimated by nonlinear least-squares method involving minimization of the following error function:

$$\chi^2 = \frac{\sum_{i=1}^{n} \left(Q_r^e - Q_r^t\right)^2}{n} \tag{15}$$

where Q_r^e is the measured relative quantum yield, Q_r^t is the relative quantum yield calculated by numerical integration of Eqs. (9)–(13), n is the number of experimental points (i.e., the number of acceptor concentrations). The data fitting procedure yielded χ^2 values not exceeding 3.7×10^{-3}. The axial depolarization factors $\langle d_D^x \rangle$ and $\langle d_A^x \rangle$ were derived from anisotropy measurements of the lipid-bound dyes. The r_D value was found to be 0.07 and the fundamental anisotropy of the anthrylvinyl fuorophore was taken as 0.08 [28]. The r_A values

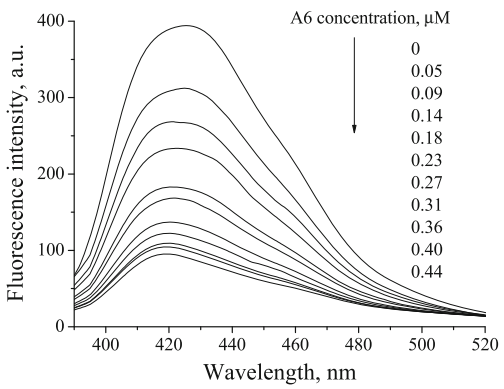

Fig. 3 Emission spectra of AV-PC in PC liposomes (0.3 mol% AV-PC) recorded at varying concentration of the benzanthrone dye A6. Lipid concentration was 10 μM

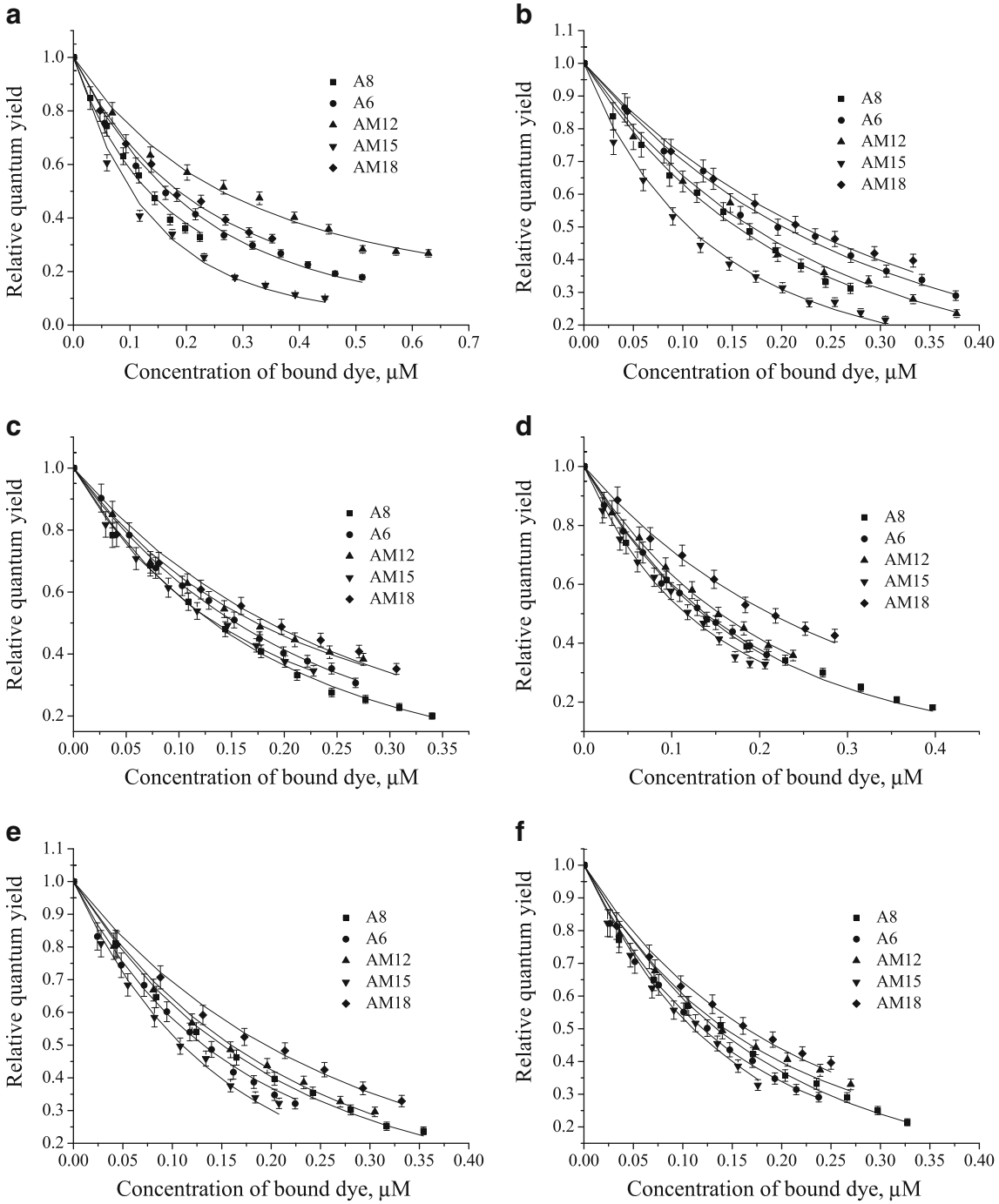

Fig. 4 Relative quantum yield of AV-PC in the dye-lipid systems as a function of bound dye concentration for PC (**a**), CL5 (**b**), CL11 (**c**), CL25 (**d**), PG20 (**e**) and PG40 (**f**) liposomes. Lipid concentration was 10 μM

of benzanthrones observed in the model membranes of various compositions are presented in Table 1. Since the preferable membrane orientation of the examined dyes is unknown, we found it reasonable to treat the experimental data on the two limiting assumptions: α_A=0 (benzanthrone plane is parallel to a lipid bilayer surface) or α_A=π/2 (benzanthrone plane is perpendicular to a lipid bilayer surface). As judged from ^{1}H NMR-spectroscopy data [29] and quenching of AV fluorescence by iodide [30], anthrylvinyl fluorophope resides at the level of terminal methyl groups preferentially orienting parallel to acyl chains. This allowed us to put α_D equal to π/2. Given the possibility of both positive and negative values of $\langle d_D^x \rangle$ and $\langle d_A^x \rangle$ all possible combinations of the signs of these parameters were considered in the data fitting.

Shown in Table 2 are the lower and upper boundaries of benzanthrone distance from the membrane midplane

Table 2 Limiting values for benzanthrone dye distance from membrane center in different lipid systems

Membrane composition	d_c, nm				
	A8	A6	AM12	AM15	AM18
α_A=0					
PC	2.0 (3.4×10^{-4})	0.6 (3.2×10^{-4})	0.5 (9.5×10^{-4})	0.6 (3.1×10^{-4})	0.9 (1.1×10^{-4})
CL5	2.0 (2.5×10^{-5})	1.4 (1.2×10^{-4})	1.6 (5.5×10^{-4})	1.6 (4.5×10^{-4})	1.5 (7.2×10^{-4})
CL11	2.0 (2.4×10^{-4})	1.5 (2.2×10^{-4})	1.5 (8.2×10^{-4})	1.5 (2.6×10^{-4})	1.5 (1.3×10^{-4})
CL25	2.0 (4.1×10^{-4})	1.5 (3.8×10^{-4})	1.5 (2.5×10^{-4})	1.6 (2.9×10^{-3})	1.5 (3.1×10^{-4})
PG20	2.0 (1.4×10^{-3})	1.4 (3.7×10^{-4})	1.5 (4.8×10^{-4})	1.6 (7.8×10^{-4})	1.5 (5.6×10^{-4})
PG40	2.1 (5.3×10^{-4})	1.5 (8.9×10^{-4})	1.6 (5.5×10^{-4})	1.6 (1.5×10^{-4})	1.5 (3.4×10^{-4})
α_A=π/2					
PC	2.2 (2.0×10^{-4})	1.2 (1.4×10^{-4})	0.9 (1.1×10^{-4})	1.1 (1.2×10^{-4})	1.3 (2.8×10^{-4})
CL5	2.1 (2.2×10^{-4})	1.8 (1.6×10^{-3})	1.8 (1.9×10^{-4})	2.1 (4.4×10^{-4})	1.7 (3.0×10^{-4})
CL11	2.1 (1.2×10^{-4})	1.9 (1.3×10^{-4})	1.9 (1.9×10^{-4})	1.9 (4.9×10^{-4})	1.7 (2.3×10^{-3})
CL25	2.1 (5.2×10^{-4})	1.9 (5.5×10^{-4})	1.8 (4.1×10^{-4})	2.0 (4.3×10^{-4})	1.8 (5.0×10^{-4})
PG20	2.1 (3.7×10^{-4})	1.8 (1.6×10^{-4})	1.8 (2.2×10^{-3})	2.1 (2.7×10^{-4})	1.7 (1.3×10^{-4})
PG40	2.1 (6.7×10^{-4})	1.9 (1.6×10^{-4})	1.9 (5.3×10^{-4})	2.1 (3.7×10^{-3})	1.8 (3.7×10^{-4})

Shown in parentheses are χ^2 values for each data fit

providing the best fit of the experimental FRET profiles. The separation of A8 from bilayer center proved to lie between 2 nm and 2.2 nm, regardless of the membrane composition. Taking into consideration the time-averaged transbilayer distributions of the lipid structural groups [31], it can be assumed that A8 is located at lipid-water interface in the vicinity of phosphocholine moiety. In the meantime, A6, AM12, AM15 and AM18 seem to penetrate into hydrophobic region of PC bilayer, with limiting separations from the membrane center being *ca*. 0.6–1.2 nm, 0.5–0.9 nm, 0.6–1.1 nm and 0.8–1.3 nm, respectively.

Importantly, the observed tendencies correlate rather well (correlation coefficient *ca.* 0.87) with the lipophilicity of benzanthrones evaluated using the resources of Virtual Computational Chemistry Laboratory (http://www.vcclab.org). As seen in Table 1, A8 displays the lowest lipophilicity, *ca.* 4.2, while for the other dyes under study this parameter ranges between 5.7 and 7.2. Furthermore, it appeared that inclusion of CL and PG into PC bilayer induces substantial relocation of benzanthrone dyes closer to the membrane surface even at rather small concentrations of anionic lipids. Accordingly, in the charged lipid membranes these dyes tend to reside in the vicinity of carbonyl groups (d_c=1.4–1.5 nm) or glycerol backbone (d_c=1.7–1.8 nm).

A question arises, why the changes in physicochemical properties of lipid bilayer induced by addition of CL and PG do not affect the localization of A8, despite high structural similarity of the examined compounds? As there exists a steep transmembrane gradient of polarity—dielectric constant changes from 80 to 2 while going from bilayer surface to its acyl chain core [32]. It can be supposed that the uncharged dye A8 with its polar carbonyl group and non-polar rest of the molecule tends to occupy a certain equilibrium position corresponding to free energy minimum with regards to this gradient. However, electrostatic factors seem to be insufficient for promoting the probe relocation in response to the alterations in bilayer composition. The change of the probe location and orientation in the ground state is hardly probable due to its small ground state dipole moment (*ca*. 4.5 D), while relocation in the excited state can be ruled-out because of the observed previously strong red-edge effect [11] demonstrating the absence of dipole relaxation dynamics. It is also worth noting that among the dyes under investigation only A8 displays substantial REES.

As seen in Table 1, addition of the anionic lipids significantly decreases the partition coefficients of A6, AM12, AM15 and AM18. Moreover, as judged from the recovered separations between benzanthrones and membrane center (Table 2), incorporation of PG and CL into PC bilayer is followed by "squeezing" these dyes out to membrane surface. Among the factors that could be responsible for the observed effects, the most essential seems to be CL- and PG-induced structural reorganization of lipid bilayer, which may cause relocation and reorientation of the probe. To exemplify, recent data on giant unilamellar vesicles indicates that Prodan and Laurdan do not have any preferential orientation in fluid-phase membranes, while in liquid-ordered and gel-phase membranes they adopt a constrained vertical orientation [33]. Kusube et al. showed that the changes in hydrostatic pressure may substantially alter membrane location of Prodan [34]. Modulating effect of cholesterol on Prodan and Nile Red bilayer penetration ability has been previously reported [35, 36]. Fluorophore relocation upon modification of membrane properties was also proposed for NBD derivatives [37] and 4′-

dimethylamino-3-hydroxyflavone [38]. Therefore, to interpret the observed differences in calculated d_c values the influence of CL and PG on lipid bilayer structure should be considered.

The grazing incidence diffraction measurements revealed that incorporation of tetramyristoyl cardiolipin into PC monolayer has significant ordering effect even at small CL concentrations [39]. This observation is in agreement with recent monolayer study suggesting that the order of PC hydrocarbon chains increases upon bovine heart CL inclusion [40]. Moreover, as expected, this condensing effect is more pronounced when the monolayers are spread on a subphase containing 150 mM NaCl [40]. Similar results were later reported for monolayers from bovine heart CL mixtures with PC and PE [41]. However, these findings are still a matter of controversy, since fluorescence anisotropy [42] measurements indicate that inclusion of up to 20 mol% CL in PC bilayer does not change bilayer fluidity. In the meantime, stabilizing effect of CL on lipid bilayer has been reported by Shibata et al. [43]. On the basis of FTIR data, the authors hypothesized that CL is capable of enhancing the hydration of ester's C = O groups and inducing cooperative changes in PC headgroups [43]. These changes were assumed to involve displacement of the N^+ end of P-N dipole toward orientation more parallel to the membrane surface, thereby resulting in rearrangement of water bridges at the bilayer surface and stabilization of the intermolecular hydrogen-bonded network including hydrational water. The stability of this network was found to be influenced by the charged moiety and the ester's carbonyl group of cardiolipin [43]. It is noted that the changes in hydration extent may considerably affect molecular organization of a lipid bilayer. In particular, increase of water content in headgroup region was reported to modify the alignment of choline-phosphate dipole and lateral packing of hydrocarbon chains [44]. Moreover, as follows from ^{2}H NMR spectroscopic studies, the presence of CL in PC bilayers alters the orientation and mobility of adjacent choline headgroups, most probably due to the interactions between positively charged quaternary PC nitrogen with the negatively charged CL phosphates [45, 46]. Interestingly, similar effect was observed for PC:PG bilayer [47, 48]. Likewise, it was found that PG induces a much denser packing of chain atoms in the near-the interface region of hydrophobic core of the mixed bilayers compared with pure PC [49] and exerts a stabilizing influence on zwitterionic bilayers [50]. All these rationales led us to suppose that the ability of CL and PG to change the conformation and dynamic of choline headgroup, along with their tendency to form more stable and condensed bilayers, could affect the molecular organization of model membranes in such a manner that the thermodynamically favorable location of the examined benzanthrone dyes becomes less buried.

To summarize, in the present study we examined Förster resonance energy transfer between anthrylvinyl-labeled phosphatidylcholine as a donor and benzanthrone moiety as an acceptor, to obtain quantitative information about the location of novel benzanthrone dyes in the model membranes composed of phosphatidylcholine and varying proportions of cardiolipin and phosphatidylglycerol. It was found that disposition of benzanthrone dyes in the lipid bilayer depends on membrane composition. Inclusion of anionic lipids CL and PG into PC bilayer forces benzanthrone dyes to shallower membrane location. These findings may prove of value in future studies involving benzanthrone dyes for probing complex biological membranes.

Acknowledgments This work was supported by the grant from Fundamental Research State Fund (project number F.54.4/015) and CIMO Fellowship (OZ).

References

1. Dobretsov G, Dmitriev V, Pirogova L, Petrov V, Vladimirov Y (1978) 4-Dimethylaminochalcone and 3-methoxybenzanthrone as fluorescent probes to study biomembranes. III Relationship between state of hydration shell of membrane and state of phospholipids. Stud Biophys 71:189–196
2. Yang X, Liu W-H, Jin W-J, Shen G-L, Yu R-Q (1999) DNA binding studies of a solvatochromic fluorescence probe 3-methoxybenzanthrone. Spectrochim Acta A 55:2719–2727
3. Kirilova E, Kalnina I (2010) 3-isopropyloxy-6-morpholino-2-phenylphenalen-1-one as lipophilic fluorescent probe for lymphocyte investigations. Appl Biochem Biotechnol 160:1744–1751
4. Kalnina I, Klimkane L, Kirilova E, Toma M, Kizane G, Meirovics I (2007) Fluorescent probe ABM for screening gastrointestinal patient's immune state. J Fluoresc 17:619–625
5. Gorbenko G, Trusova V, Kirilova E, Kirilov G, Kalnina I, Vasilev A, Kaloyanova S, Deligeorgiev T (2010) New fluorescent probes for detection and characterization of amyloid fibrils. Chem Phys Lett 495:275–279
6. Vus K, Trusova V, Gorbenko G, Kirilova E, Kirilov G, Kalnina I, Kinnunen P (2012) Novel aminobenzanthrone dyes for amyloid fibril detection. Chem Phys Lett 532:110–115
7. Kirilova E, Kalnina I, Kirilov G, Meirovics I (2008) Spectroscopic study of benzanthrone 3-*N*-derivatives as new hydrophobic fluorescent probes for biomolecules. J Fluoresc 18:645–648
8. Refat M, Aqeel S, Grabtchev I (2004) Spectroscopic and physicochemical studies of charge-transfer complexes of some benzanthrone derivatives "Luminophore Dyes" with iodine as σ-acceptor. Can J Anal Sci Spectrosc 49:258–265
9. Grabchev I, Bojinov V, Moneva I (1998) Functional properties of azomethine substituted benzanthrone dyes for use in nematic liquid crystals. J Mol Struct 471:19–25
10. Lakowicz J (1999) Principles of fluorescent spectroscopy, 2nd edn. Plenum Press, New York
11. Trusova V, Kirilova E, Kalina I, Kirilov G, Zhytniakivska O, Fedorov P, Gorbenko G (2012) Novel benzanthrone aminoderivatives for membrane studies. J Fluoresc 22:953–959
12. Zhytniakivska O, Trusova V, Gorbenko G, Kirilova E, Kalnina I, Kirilov G, Kinnunen P (2014) Newly synthesized benzanthrone derivatives as prospective fluorescent membrane probes. J Lumin 146:307–313
13. Fung B, Stryer L (1978) Surface density determination in membranes by fluorescence energy transfer. Biochemistry 17:5241–5248

14. Bergelson L, Molotkovsky J, Manevich Y (1985) Lipid-specific probes in studies of biological membranes. Chem Phys Lipids 37: 165–195
15. Molotkovsky J, Dmitriev P, Nikulina L, Bergelson L (1979) Synthesis of new fluorescent labeled phosphatidylcholines. Bioorg Khim 5:588–594
16. Gonta S, Utinans M, Kirilov G, Belyakov S, Ivanova I, Fleisher M, Savenkov V, Kirilova E (2013) Fluorescent substituted amidines of benzanthrone: synthesis, spectroscopy and quantum chemical calculations. Spectrochim Acta A 101:325–334
17. Bulychev A, Verchoturov V, Gulaev B (1988) Current methods of biophysical studies. Vyschaya shkola, Moscow
18. Santos N, Prieto M, Castanho M (2003) Quantifying molecular partition into model systems of biomembranes: an emphasis on optical spectroscopic methods. Biochim Biophys Acta 1612:123–135
19. Ivkov V, Berestovsky G (1981) Dynamic structure of lipid bilayer. Nauka, Moscow
20. Gorbenko G, Kinnunen P (2013) FRET analysis of protein-lipid interactions. Springer Ser Fluoresc Fluorescent Methods Study Biol Membr 13:115–140
21. Ardail D, Privat J, Egretcharlier M, Levrat C, Lerme F, Louitson P (1990) Mitochondrial contact sites—lipid composition and dynamics. J Biol Chem 265:18797–18802
22. Flewelling R, Hubbel W (1986) The membrane dipole potential in a total membrane potential model. Application to hydrophobic ion interaction with membranes. Biophys J 49:541–552
23. Ceve G (1990) Membrane electrostatics. Biochim Biophys Acta 1031:311–382
24. Franklin J, Cafiso D (1995) Internal electrostatic potentials in bilayers: measuring and conrolling dipole potentials in lipid vesicles. Biophys J 65:289–299
25. Zhao G-J, Han K-l (2012) Hydrogen bonding in the electronic excited state. Acc Chem Res 45:404–413
26. Zhao G-J, Liu J-Y, Zhou L-C, Han K-L (2007) Site-selective photoinduced electron transfer from alcoholic solvents to the chromophore facilitated by hydrogen bonding: a new quenching mechanism. J Phys Chem B 111:8940–8945
27. Zhang M-X, Zhao G-J (2012) Modification of n-type organic semiconductor performance of perylene diimides by substitution in different positon: two-dimensional π-stacking and hydrogen bonding. ChemSusChem 5:879–887
28. Johansson L, Molotkovsky J, Bergelson L (1990) Fluorescence properties of anthrylvinyl lipid probes. Chem Phys Lipids 53: 185–189
29. Molotkovsky J, Manevich E, Gerasimova E, Molotkovskaya I, Polessky V, Bergelson L (1982) Differential study of phosphatidylcholine and sphingomyelin in human high-density lipoproteins with lipid-specific fluorescent probes. Eur J Biochem 122:573–579
30. Boldyrev I, Zhai X, Momsen M, Brockman H, Brown R, Molotkovsky J (2007) New BODIPY lipid probes for fluorescence studies of membranes. J Lipid Res 48:1518–1532
31. Wiener M, White S (1992) Structure of a fluid dioleoylphosphatidylcholine bilayer determined by joint refinement of X-ray and neutron diffraction data. Biophys J 61:437–447
32. Epand R, Kraaychenhof R (1999) Fluorescent probes to monitor membrane interfacial polarity. Chem Phys Lipids 101:57–64
33. Bagatolli L (2006) To see or not to see: lateral organization of biological membranes and fluorescence microscopy. Biochim Biophys Acta 1758:1541–1556
34. Chong P (1988) Effects of hydrostatic pressure on the location of Prodan in lipid bilayers and cellular membranes. Biochemistry 27: 399–404
35. Bondar O, Rowe E (1999) Preferential interactions of fluorescent probe Prodan with cholesterol. Biophys J 76:956–962
36. Mukherjee S, Raghuraman H, Chattopadhyay A (2007) Membrane localization and dynamics of Nile Red: effect of cholesterol. Biochim Biophys Acta 1768:58–66
37. Alakoskela JMI, Kinnunen PKJ (2001) Probing phospholipid main phase transition by fluorescence spectroscopy and a surface redox reaction. J Phys Chem B 105:11294–11301
38. Klymchenko A, Duportail G, Demchenko A, Mely Y (2004) Bimodal distribution and fluorescence response of environment-sensitive probes in lipid bilayers. Biophys J 86:2929–2941
39. Etienne F, Roche Y, Peretti P, Bernard S (2008) Cardiolipin packing ability studied by grazing incidence X-ray diffraction. Chem Phys Lipids 152:13–23
40. Nichols-Smith S, The S-Y, Kuhl T (2004) Thermodynamic and mechanical properties of model mitochondrial membranes. Biochim Biophys Acta 1663:82–88
41. Domenech O, Sanz F, Montero M, Hernandez-Borell J (2006) Thermodynamic and structural study of the main phospholipids components comprising the mitochondrial inner membrane. Biochim Biophys Acta 1758:213–221
42. Chen Q, Li Q (2001) Effect of cardiolipin on proton permeability of phospholipid liposomes: the role of hydration at the lipid-water interface. Arch Biochem Biophys 389:201–206
43. Shibata A, Ikawa K, Shimooka T, Terada H (1994) Significant stabilization of the phosphatidylcholine bilayer structure by incorporation of small amounts of cardiolipin. Biochim Biophys Acta 1192: 71–78
44. Sparrman T, Westlund P (2003) An NMR line shape and relaxation analysis of heavy water powder spectra of the L-alpha, L-beta and P-beta phases in the DPPC/water system. Phys Chem Chem Phys 5: 2114–2121
45. MacDonald P, Seelig J (1987) Calcium binding to cardiolipin-phosphatidylcholine bilayers as studied by deuterium nuclear magnetic resonance. Biochemistry 26:6292–6298
46. Pinjeiro T, Andeezei A, Duralski A, Watts A (1994) Phospholipid headgroup-headgroup electrostatic interactions in mixed bilayers of cardiolipin with phosphatidylcholines studied by ^{2}H NMR. Biochemistry 33:4896–4902
47. MacDonald P, Seelig J (1987) Calcium binding to mixed phosphatidylglycerol-phosphatidylcholine bilayers as studied by deuterium nuclear magnetic resonance. Biochemistry 26:1231–1240
48. Scherer P, Seelig J (1987) Structure and dynamics of the phosphatidylcholine and phosphatidylcholine headgroup in L-M fibroblasts as studied by deuterium nuclear magnetic resonance. EMBO J 6:2915–2922
49. Murzyn K, Rog T, Pasenkiewier-Gierula M (2005) Phosphatidylethanolamine-phosphatidylglycerol bilayer as a model of the inner bacterial membrane. Biophys J 88:1091–1103
50. Tari A, Huang L (1989) Structure and function relationship of phosphatidylglycerol in the stabilization of the phosphatidylethanolamine bilayer. Biochemistry 28:7708–7712